J. Anat. (1989), **162**, pp. 67–82
With 7 figures
Printed in Great Britain

The effect of various levels of intraocular pressure on the rat aqueous outflow system*

P. G. McMENAMIN AND M. J. AL-SHAKARCHI
Department of Anatomy, University of Glasgow, Glasgow G12 8QQ

(*Accepted* 19 *April* 1988)

INTRODUCTION

Investigations into the normal and abnormal mechanisms of aqueous humour drainage in the eye are motivated by an inadequate understanding of the aetiology and pathogenesis of many forms of glaucoma. Experimental studies of the functional morphology of the human outflow system are hampered by the paucity of fresh normal tissue. Higher primates have been preferred as experimental models due to the morphological similarity of the iridocorneal angle tissues and ciliary body (Rohen, 1982). However, the problems of expense and availability have prompted several groups to use non-primates as animal models including hamsters (Ohnishi & Tanigushi, 1983), domestic cattle (Anderson, Wang & Epstein, 1980), rabbit (Hernandez *et al.* 1983; Grierson *et al.* 1986), cat (Richardson, Marks, Ausprunk & Miller, 1985) and other species.

The morphology of the aqueous outflow system of most other species differs from primates in several respects: a well-developed accommodating apparatus is absent; the filtering tissue does not consist of connective tissue lamellae covered by trabecular endothelial cells but, in contrast, has a reticular appearance; lastly a single circular aqueous drainage channel analogous to the canal of Schlemm (sinus venosus sclerae) is usually absent. In many species the aqueous is drained by a variable number of small collecting channels or a subscleral (angular aqueous) plexus (Tripathi & Tripathi, 1972; Rohen, 1982), which are not confluent circumferentially.

Little interest has been shown in the rat eye since Van der Zypen (1977) described it as sharing many features of the primate outflow system, especially a canal of Schlemm, which may make it a suitable model for experimental studies of aqueous humour drainage. Presumably the obvious problem of size has deterred further investigations of this species, although Remé and co-workers have utilised the rat in developmental studies of the angular tissues (Remé, Urner & Aeberhard, 1983*a*, *b*).

The response of the primate outflow system to changes in intraocular pressure (IOP) is well documented by various groups (Johnstone & Grant, 1973; Grierson & Lee, 1974, 1975*a*, *b*; Kayes, 1975; Svedbergh, 1976). At increased IOPs the corneoscleral meshwork and cribriform layer become distended and the incidence of giant vacuoles in the lining endothelium of Schlemm's canal increases (see Lee, Grierson & McMenamin, 1982 for review). In the only study of the effects of various levels of IOP on a non-primate outflow system, Grierson *et al.* (1986) found the response in the rabbit eye less convincing than that in primates. They concluded that, due to variation

* Reprint requests to Dr P. G. McMenamin, Department of Anatomy and Human Biology, The University of Western Australia, Nedlands, Perth 6009, Western Australia.

in the organisation of the rabbit angular aqueous plexus of vessels, this species was far less suitable for quantitative studies of giant vacuoles than primates.

The aim of the present study was to determine whether the rat aqueous outflow system responds to alterations in IOP in a similar fashion to that of primates, and thereby to evaluate the suitability of this species as a model for future studies of experimentally induced aqueous outflow obstruction.

MATERIALS AND METHODS

Experimental tissues

Twenty five mature female Swiss albino rats weighing between 230 and 320 g (mean 259 g) were used in the present investigation. The animals were anaesthetised with sodium pentobarbitone (30 mg per ml) via a tail vein to a level at which the corneal reflex was suppressed.

Each rat was placed in a stereotaxic frame in the prone position. A 30 gauge needle was inserted gently through the supranasal cornea into the anterior chamber of one eye with the aid of a micromanipulator and dissecting microscope. The needle was attached to a reservoir by means of flexible 1 mm bore polythene tubing. The reservoir contained 3% cacodylate-buffered glutaraldehyde (pH 7·4) to which a few drops of fluorescein had been added to act as a marker dye.

Groups of five eyes were fixed at each of the following pressures: 0, 10, 20, 30, 40 mmHg. Intracameral fixation at all pressure levels, except 0 mmHg, was obtained by maintaining the meniscus of the reservoir at a predetermined height above the eye. Once cannulated, the eye was opened to the reservoir for 10 minutes, after which the animal was killed by an overdose of anaesthetic. Intracameral fixation was continued for a further 20 minutes, before the eye was enucleated and immersed in fixative. At low pressures (10 and 20 mmHg), fixative entered the anterior chamber slowly during the first 10 minutes whilst at higher pressures entry was more rapid. At all pressures fixative was seen to enter more quickly upon death. Intracameral fixation was not possible at 0 mmHg. Therefore in five animals one eye was cannulated and the tubing left open to atmospheric pressure for 10 minutes. The eyes were then quickly enucleated and immersed in fixative.

Control tissues

Normal mature female Swiss albino rats provided control tissue. The eyes were either enucleated and immersion-fixed after the animals were killed (by either a sodium pentobarbitone or an ether overdose) or enucleated after cardiac perfusion with glutaraldehyde.

All eyes were divided at the equator, the lens carefully removed and five limbal blocks were dissected from the anterior segment. One block from each eye was taken for scanning electron microscopy (SEM) and four for conventional transmission electron microscopy (TEM). Tissue for TEM was osmicated and processed for embedding in Araldite in the standard fashion.

Meridional semithin sections (1–2 μm) were stained with toluidine blue. Each block was sampled randomly at two different depths, thus providing a total of 8 sections per eye from the circumference of the limbus. Ultrathin sections (60–90 nm) were taken from representative blocks within each eye and stained with uranyl acetate and lead citrate. These were then examined in a Philips 301 transmission electron microscope. Tissue for SEM was critical-point dried, coated with gold and examined in a JEOL JSM T300.

Light microscopic quantitative study

The following features of the rat aqueous outflow system were assessed in 8 semithin sections from each eye with the use of the × 100 objective (oil immersion) and a calibrated eyepiece graticule: (i) the length of Schlemm's canal; (ii) the incidence of nuclei and giant vacuoles in the lining endothelium of Schlemm's canal (Grierson & Lee, 1977*a*) expressed as both inner wall giant vacuoles and total giant vacuoles (inner wall plus outer wall); (iii) the incidence of detachment of the lining endothelium from the underlying trabecular tissue and the approximate length of endothelium involved. All sections were coded during the quantitative study.

Results from each of the 8 sections were used to calculate the mean and standard deviation of each of the above features for each eye. The means from the 5 eyes at each pressure level were pooled and a group mean and standard deviation calculated. The results were statistically analysed as a generalised linear model using the Poisson distribution. The deviances were treated as chi-squared with the appropriate degrees of freedom.

RESULTS

The normal morphology of the rat chamber angle

The tissues of the aqueous outflow system in the rat, as in most vertebrates, lie at the corneoscleral limbus of the eye at the apex of the iridocorneal or anterior chamber angle (Fig. 1*a*, *b*). The rat eye does not possess a well-developed ciliary muscle and the ciliary body thus comprises only a few longitudinally orientated smooth muscle fibres externally and the ciliary ridges or processes internally (Fig. 1*a*). The ciliary processes are convoluted, irregularly shaped, highly vascular projections covered by a double layer of columnar or cuboidal epithelium (Fig. 1*a*). They are relatively anteriorly placed in comparison to the primate eye and arise either from the prelenticular part of the ciliary body or from the posterior aspect of the iris. A pars plana ciliaris is not present in this species and the retina ends abruptly at the posterior margin of the ciliary processes (Fig. 1*a*). The anterior chamber angle recess or ciliary cleft intervenes between the inner aspect of the corneoscleral limbus externally and the ciliary processes/iris root internally (Fig. 1*a*, *b*). The specialised connective tissue that fills the angle recess and, in particular, that which is found internal to the shallow scleral sulcus is analogous to the trabecular meshwork in primates. The trabeculae comprise 2–6 perforated collagenous sheets or lamellae orientated approximately parallel to the canal of Schlemm (Fig. 1*a–c*). Those nearest the anterior chamber, the so-called pectinate ligaments, which are often thicker, bridge the gap between the anterior extremity of the trabecular tissue (the termination of Descemet's membrane) and the connective tissue of the iris stroma. It is the slightly larger spaces behind these pectinate ligaments that are referred to as the spaces of Fontana (Fig. 1*a–c*).

The ultrastructural appearance of the trabeculae (Fig. 2) is similar to that previously described in primates. They consist of a collagen core and elastic-like fibres surrounded by an incomplete basal lamina and lined by flattened trabecular endothelial cells (TECs). The trabecular tissue directly beneath the inner wall of Schlemm's canal lacks the organisation of trabeculae and is analogous to the cribriform layer of primates.

Anterior to the few ciliary muscle fibres, within a shallow sulcus, lies a single endothelial lined channel, the canal of Schlemm, 50–150 μm in length and 5–25 μm wide (Fig. 1*a–c*). The lining endothelium of the outer wall of this channel rests upon

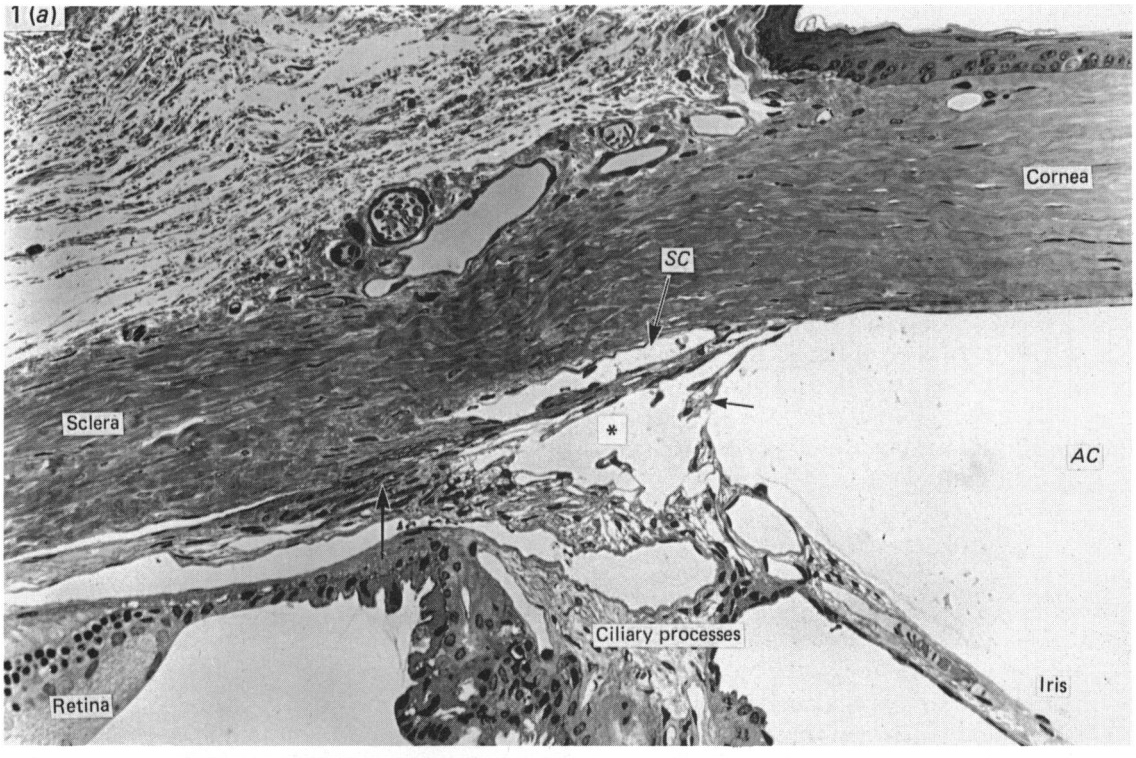
1 (a)
Cornea
SC
Sclera
*
AC
Ciliary processes
Iris
Retina

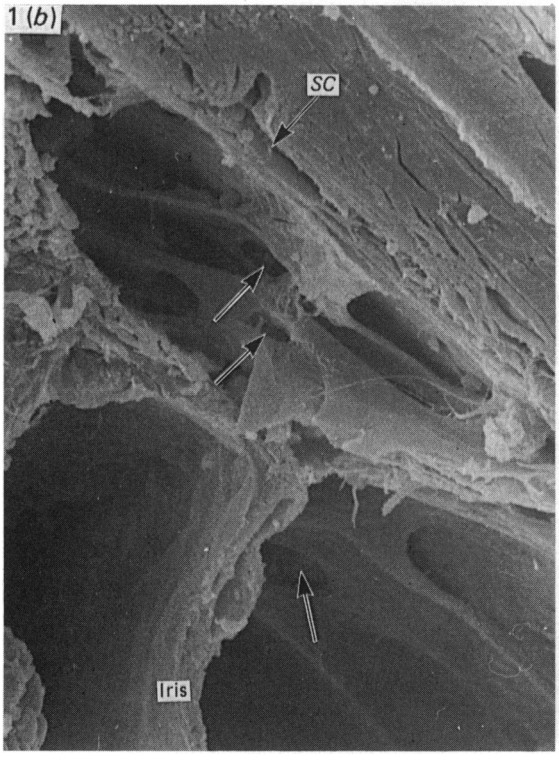
1 (b)
SC
Iris

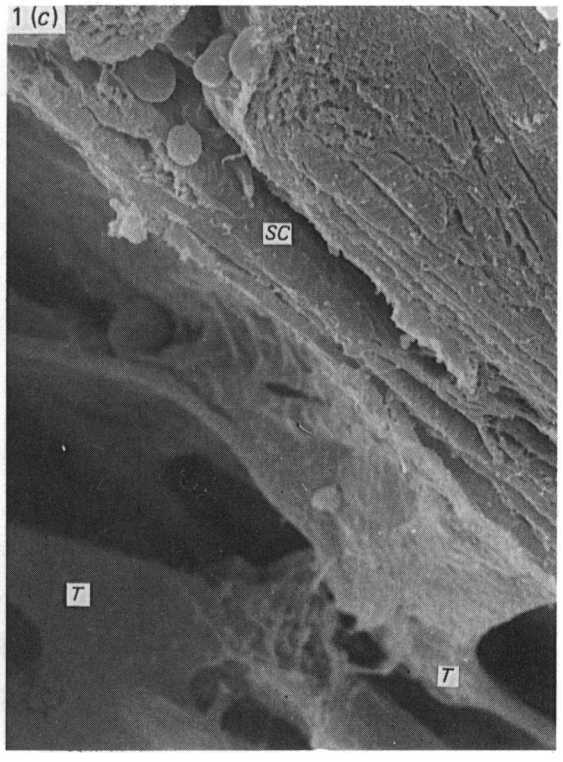
1 (c)
SC
T
T

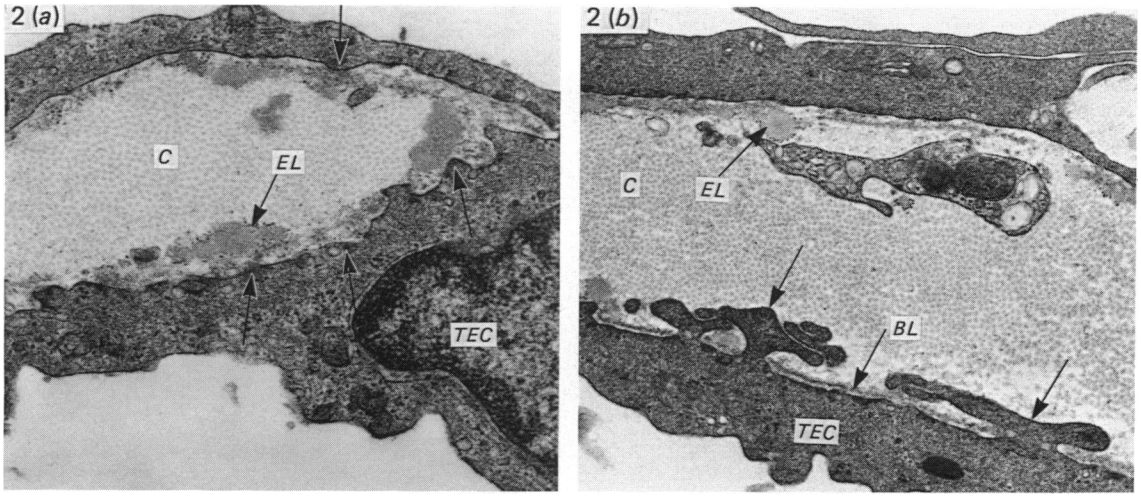

Fig. 2(*a–b*). Transmission electron micrographs of trabeculae in the normal Swiss albino rat which demonstrate the arrangement of the trabecular endothelial cells (*TEC*) surrounding the matrix of collagen (*C*) which makes up the bulk of the trabeculum. Elastic-like fibres (*EL*) and basal lamina material (*BL*) are also usually identifiable. Densifications of cytoplasmic filaments together with cytoplasmic pegs (arrows) are presumably important in maintaining adhesion between the TECs and the extracellular matrix.) (*a*) ×25000; (*b*) ×19000.

dense corneoscleral tissue. On the inner aspect the endothelium separates the lumen from the connective tissue that forms the trabecular meshwork and the aqueous-containing intertrabecular spaces and spaces of Fontana, which are in direct continuity with the anterior chamber (Fig. 1 *a–c*). The lining endothelium of Schlemm's canal consists of a very attenuated monolayer of endothelial cells, united by tight junctions, resting upon an incomplete basal lamina. The outer wall nuclei are flattened, while those of the inner wall are more prominent and are frequently indented. Numerous peg-like processes attach the endothelium of the inner wall to the underlying cells and extracellular matrix of the cribriform layer. These are less frequent on the outer wall. Membrane-bound intracellular vacuoles (1–10 μm) are present in the lining endothelium. These are identical to those previously described in other species. Many possess openings or pores on the trabecular aspect. Pores on the luminal aspect are rarer.

Collector channels, which form a communication between the canal of Schlemm on the inner aspect of the limbus and episcleral veins externally, are occasionally noted passing through the corneoscleral tissue.

Low intraocular pressure (0 *and* 10 *mmHg*)

At 0 mmHg the ciliary cleft or anterior chamber angle was compressed and the iris was occasionally in contact with the posterior surface of the cornea. The spaces of Fontana were collapsed and the connective tissue stroma of the ciliary body and iris

Fig. 1.(*a–c*). Light (*a*) and scanning electron micrographs (*b–c*) to illustrate the normal appearance of the iridocorneal angle in the Swiss albino rat. In (*a*) the few smooth muscle fibres which correspond to the ciliary muscle in primates are indicated (large arrow). The pectinate ligaments (small arrow) partially separate the anterior chamber (*AC*) from the spaces of Fontana (*). Note the single endothelial lined canal of Schlemm (*SC*). Scanning electron microscopy (*b–c*) clearly demonstrates that the trabeculae (*T*) consist of perforated lamellae (arrows) lying internal to Schlemm's canal. (*a*) ×260; (*b*) ×560; (*c*) ×1800.

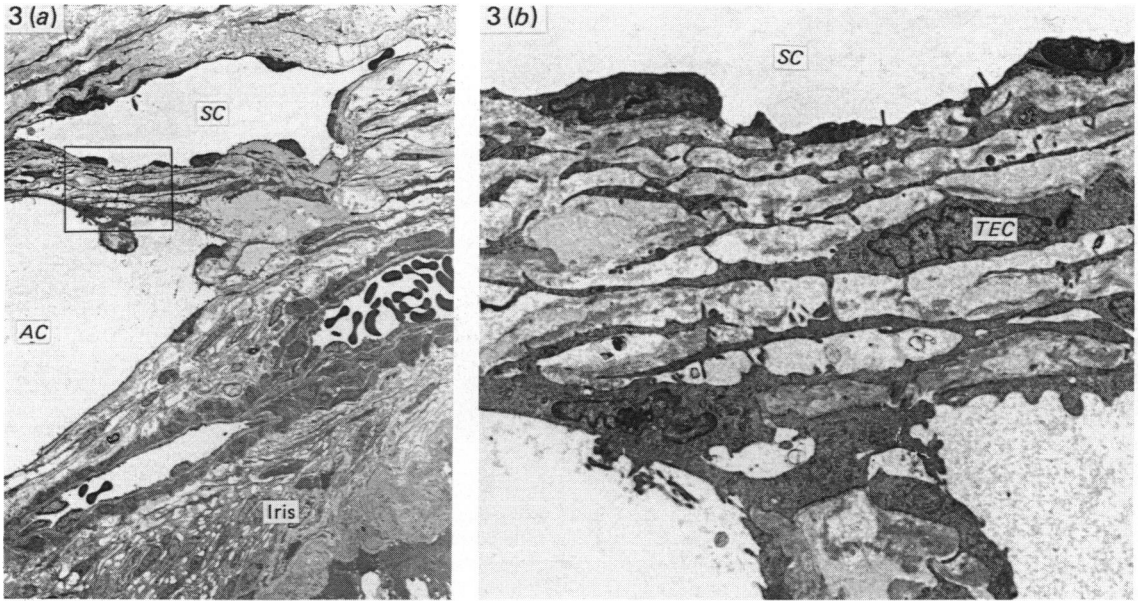

Fig. 3(*a–b*). Electron micrographs of the outflow system at 0 mmHg. (*a*) illustrates the compact iris base and outflow system, the dilated canal of Schlemm (*SC*) and the paucity of giant vacuoles. At higher magnification (*b*) there is little evidence of fluid-filled intertrabecular spaces. *AC*, anterior chamber; *TEC*, trabecular endothelial cell. (*a*) ×700; (*b*) ×4000.

base formed a compact mass against the trabecular meshwork (Fig. 3*a*). The outer layers of the meshwork were compressed, and few electron-lucent spaces were detectable at the ultrastructural level (Fig. 3*b*). The canal of Schlemm at this pressure and at 10 mmHg was dilated and contained either refluxed blood or aqueous humour (Fig. 3*a*). The lining endothelium was flattened and often bowed inwards. Giant vacuoles were rarely identified by light microscopy at 0 mmHg and infrequently at 10 mmHg in most of the eyes. Ultrastructural examination of eyes fixed at 0 mmHg revealed only the occasional bleb in the lining endothelium, which was attached at regular intervals to the underlying cells and extracellular matrix (Fig. 3*b*). However, in one eye fixed at 10 mmHg giant vacuoles were relatively numerous (see quantitative results).

20 *mmHg*

At this pressure the angle was open and the spaces of Fontana and the intertrabecular spaces were dilated (Fig. 4*a*). The outer meshwork was more distended than in eyes fixed at lower IOPs. The lining endothelium of Schlemm's canal in most sections contained between 1 and 7 giant vacuoles, almost all on the inner wall (Fig. 4*a*); however, there was a great deal of variation in the appearance of the lining

Fig. 4(*a–c*). The rat outflow system at 20 mmHg. In (*a*) note that the tissue is distended and trabeculae (*T*) are widely separated. Higher magnification of two areas indicated in (*a*) illustrates firstly an area of detached endothelium (*b*) in which cytoplasmic linkages (arrows) with the underlying tissue have been lost. By contrast in a nearby area (*c*) giant vacuoles (*GV*) are clearly visible and the endothelial monolayer is still tethered by cytoplasmic processes to the tissue beneath (large arrows). Cell junctions in the endothelium are indicated (small arrows) together with false vacuoles or blebs (*B*). *SC*, Schlemm's canal; *CL*, cribriform layer. (*a*) ×200; (*b*) ×6000; (*c*) ×19800.

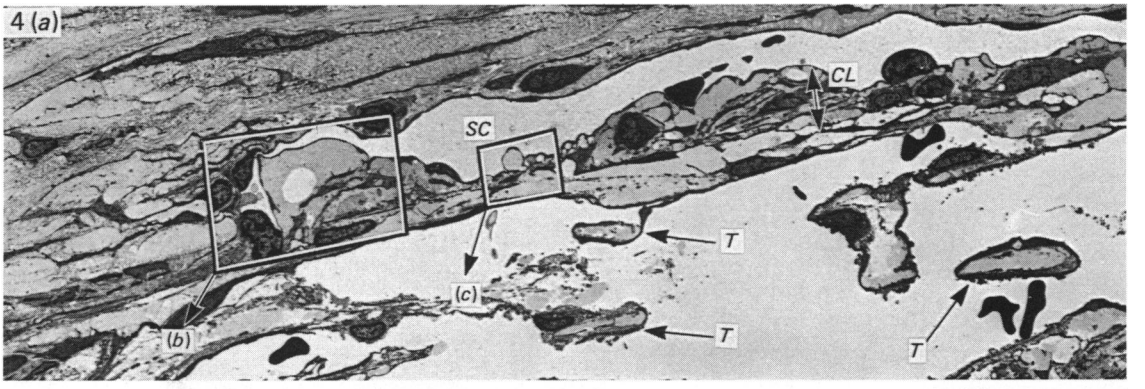
4 (a)
CL
SC
T
(c)
(b)
T
T

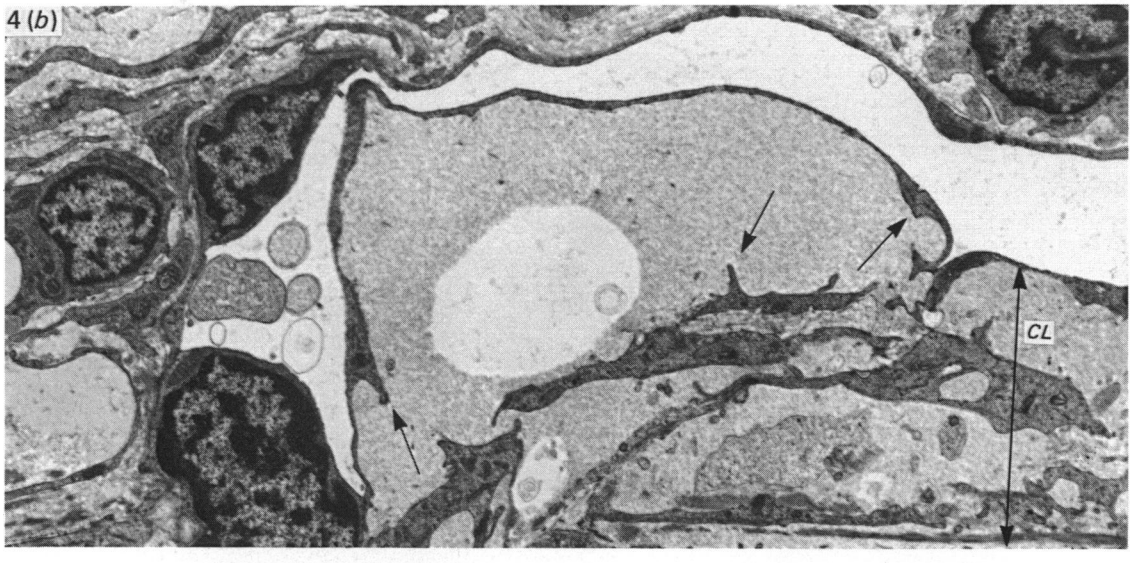
4 (b)
CL

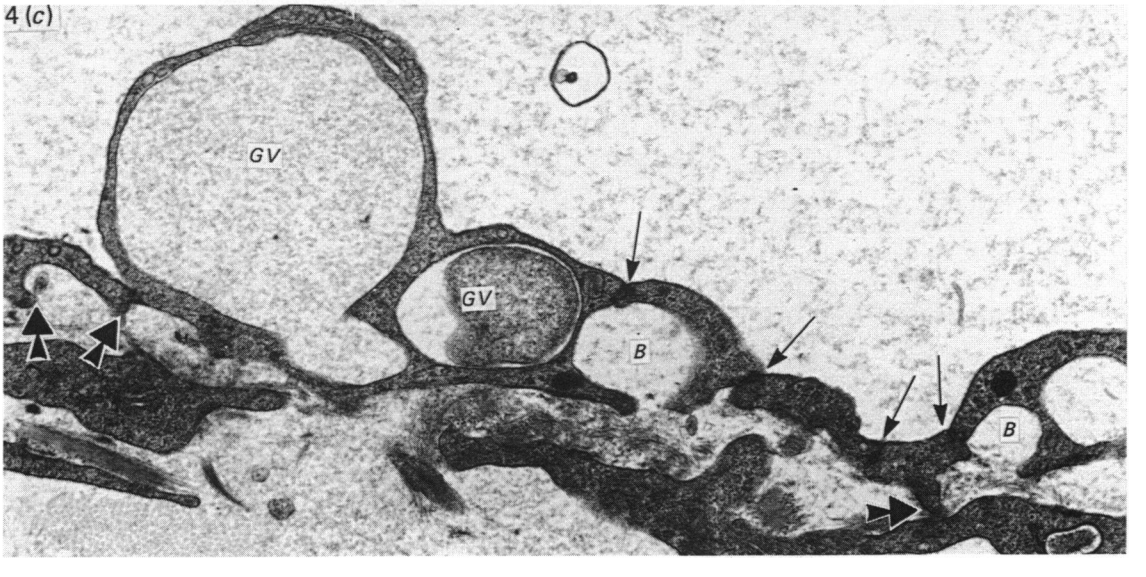
4 (c)
GV
GV
B
B

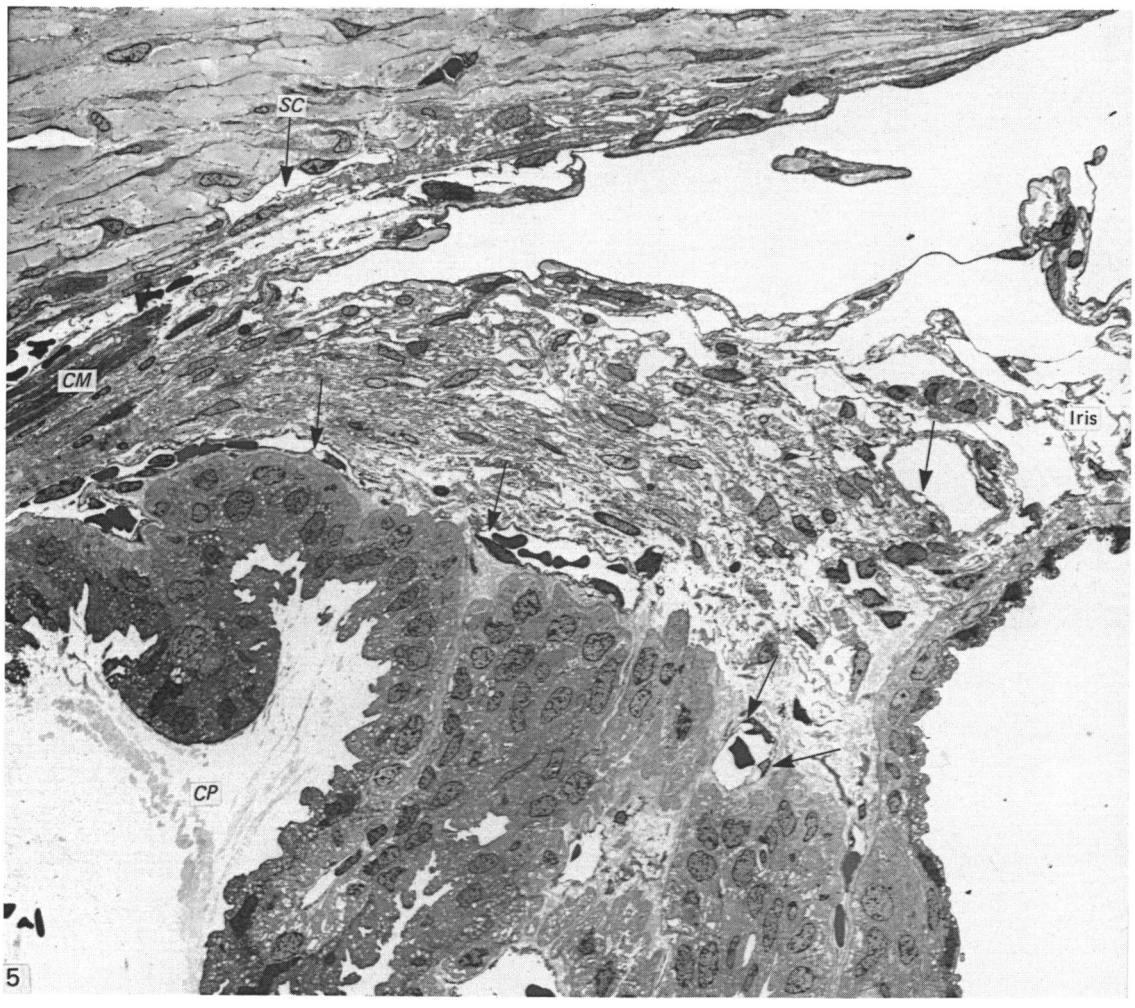

Fig. 5. Low power electron micrograph of the iridocorneal angle at 30 mmHg. A small posterior portion of Schlemm's canal (*SC*) remains patent while distension of the trabecular tissues has resulted in closure of most of the lumen. Vacuole-like structures can be seen in the lining of neighbouring vessels (arrows). *CM*, ciliary muscle; *CP*, ciliary processes. × 770.

endothelium between closely adjacent sections. In some sections short segments of the lining endothelium were occasionally detached from the underlying cribriform tissue (Fig. 4*b*). These focal detachments ballooned out into the lumen of the canal. They usually involved more than one endothelial cell. This occurred more frequently in the posterior part of the canal.

High intraocular pressures (30 *and* 40 *mmHg*)

The anterior chamber angle was open in all of the eyes fixed at these pressures. The ciliary cleft extended more posteriorly than normal in some sections and fluid-filled

Fig. 6(*a–b*). Rat aqueous outflow system at 40 mmHg. In (*a*) a large portion of the lining endothelium is detached and devoid of vacuoles. Inset – higher magnification of lost cell–cell attachments, indicated by arrows. In (*b*) by comparison the outer meshwork is distended and giant vacuoles (*GV*) are common in the wall of Schlemm's canal (*SC*). Inset – low power, showing the stretched cytoplasmic extensions (arrowheads). (*a*) × 4200 (inset × 13000); (*b*) × 14200 (inset × 1000).

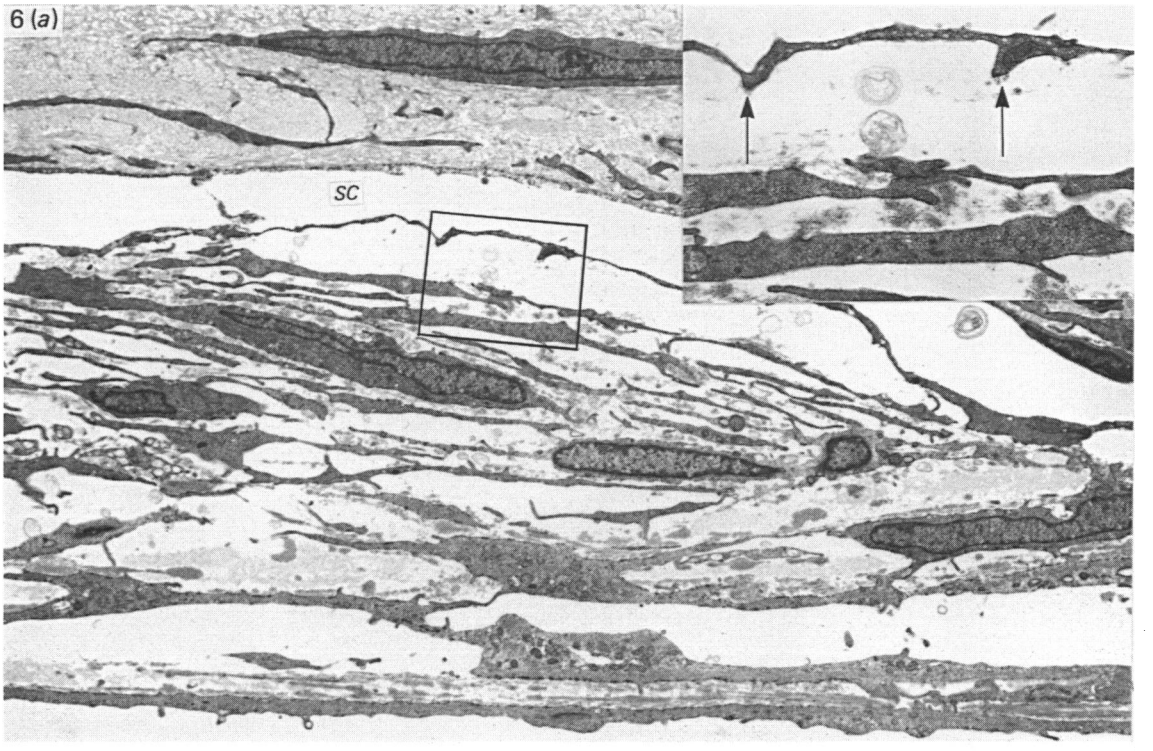
6 (*a*)
SC

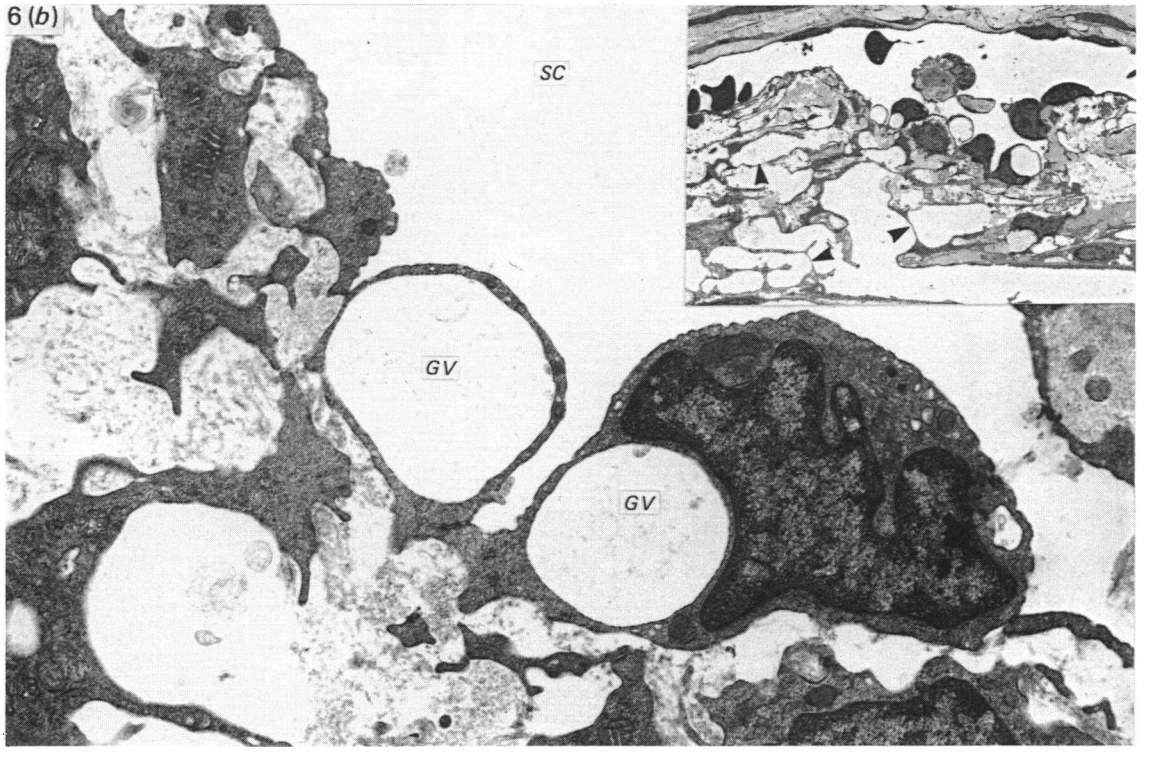
6 (*b*)
SC
GV
GV

Table 1. *Quantitative assessment of the changes in the rat outflow system at various levels of IOP (mmHg). Group means* ($\pm$ *S.D.*), n = 5

IOP (mmHg)	Length of Schlemm's canal (μm)	Number of inner wall nuclei	Number of inner wall giant vacuoles	Number of total giant vacuoles	Inner wall giant vacuoles/mm Schlemm's canal	Percentage length of detached endothelium
0	70·4 ± 16·8	1·9 ± 0·86	0·13 ± 0·18	0·13 ± 0·18	2·09 ± 2·86	1·62 ± 3·0
10	101·6 ± 26·0	3·04 ± 0·94	0·65 ± 0·9	0·83 ± 1·0	7·33 ± 9·8	2·23 ± 2·0
20	91·1 ± 8·3	2·58 ± 0·88	1·07 ± 0·62	1·35 ± 0·75	11·7 ± 4·4	9·6 ± 4·7
30	105·9 ± 16·1	2·78 ± 0·86	1·74 ± 1·16	1·97 ± 1·22	15·9 ± 8·23	7·6 ± 6·5
40	96·6 ± 30·7	2·35 ± 0·45	2·2 ± 2·67	2·63 ± 2·96	20·0 ± 18·9	11·2 ± 7·3

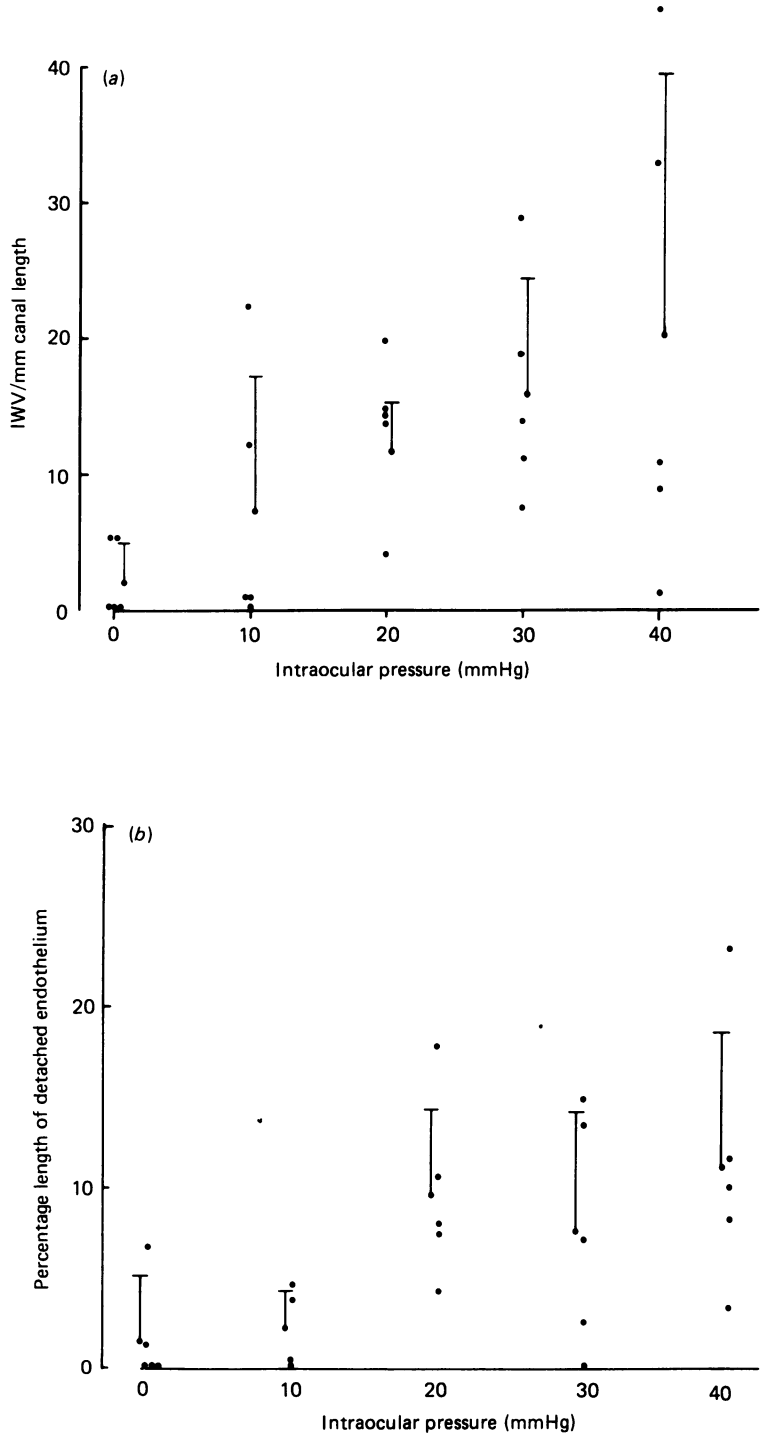

Fig. 7(*a–b*). Results of the light microscopic quantitative assessment of the rat outflow system at different levels of intraocular pressure. In (*a*) the mean numbers of inner wall vacuoles (IWV) per mm length of Schlemm's canal in each eye are plotted against IOP. In (*b*) the mean percentage length of the canal endothelium which was detached in each eye is plotted against IOP. The group means (±S.D.) are illustrated.

spaces, continuous with the distended intertrabecular spaces, appeared far back into the vascular connective tissue of the ciliary body (Fig. 5). The pectinate ligaments were stretched but intact and the cytoplasmic extensions of the TECs were still identifiable (Fig. 6*b*, inset). Signs of tissue damage to the inner layers of the meshwork, such as loss of cell-to-cell contact and denudation of trabeculae, were infrequent and disruption of the connective tissue elements was rare. The cribriform layer was distended and bowed outwards, narrowing or closing the lumen of Schlemm's canal (Figs 5, 6*a*). Focal detachment of the lining endothelium was more common than at lower pressures (Fig. 6*a*). These detachments sometimes formed large balloon-like structures which bulged into Schlemm's canal. Giant vacuoles were not detectable in any region of detached endothelium or in areas of canal closure. In the few instances in which a collector channel draining the canal was observed the outer layers of trabecular tissue and the inner wall of the canal were prolapsed into the opening. In those patent areas of canal in which the lining endothelium was not detached, giant vacuoles were observed in reasonable numbers (Fig. 6*b*). Structures resembling giant vacuoles were observed in the endothelium of several blood vessels in the iris root and ciliary body in a few eyes (Fig. 5).

Quantitative results

The results are summarised in Table 1. The mean length of Schlemm's canal ($\simeq$ 100 μm) was reasonably similar in all five groups, although in the groups fixed at 10 and 30 mmHg it was marginally higher. The mean number of inner wall nuclei per section showed no statistical trend. Few giant vacuoles were observed in the inner wall of Schlemm's canal at 0 mmHg (Fig. 7). One eye fixed at 10 mmHg had a larger number of vacuoles per section than the remainder of the group. The mean number of vacuoles per mm of Schlemm's canal (corrected using the measurement of mean canal length in each eye) at pressures of 10, 20, 30 and 40 mmHg was significantly higher than at 0 mmHg ($P < 0{\cdot}01$), although there was some variation in response within groups (Fig. 7). The percentage length of detached endothelium was significantly higher at pressures of 20, 30 and 40 mmHg than at 0 mmHg ($P < 0{\cdot}01$) (Fig. 7).

DISCUSSION

The appearance of the normal rat iridocorneal angle in the present investigation confirms the work of Van der Zypen (1977) and reaffirms his conclusions that the morphological similarity of the angle in this species to that of primates, especially the presence of a single canal of Schlemm, may make it a useful experimental model for the study of normal and abnormal mechanisms of aqueous drainage. In this context it is of special significance that in the present study we describe the iridocorneal angle of the Swiss albino rat as consisting of a few layers of well-organised trabeculae; a loosely organised cribriform layer and a single circumferential canal of Schlemm (characterised by giant vacuoles), which is drained by collector channels into the episcleral venous plexus. These features are common to all other strains investigated, namely Hooded Lister, Fisher, PVC, WAG, Wistar (personal observations) and Sprague–Dawley (Remé *et al.* 1983*a*, *b*). This arrangement of the trabecular meshwork contrasts with most non-primates, e.g. rabbits, in which the angle is filled by a reticular meshwork of cells loosely embedded in various types of collagen and proteoglycans (Tripathi & Tripathi, 1972; Rohen, 1982; Grierson *et al.* 1986). The possession of a single canal of Schlemm is unusual in a non-primate. In most other species a series of vascular loops (angular aqueous plexus) arise from the episcleral venous system and

pass through the sclera into the iridocorneal angle. The arrangement of these vessels is highly variable not only between species but also around the circumference of the angle within one eye (Ruskell, 1961; Van Buskirk, 1979; Richardson *et al.* 1985; Grierson *et al.* 1986).

The presence of giant vacuoles in the lining endothelium of Schlemm's canal in the rat has been reported previously (Tripathi & Tripathi, 1972; Van der Zypen, 1977). Although Van der Zypen considered that giant vacuoles may be a route of aqueous movement across the lining endothelium he concluded that this was carried out predominantly by micropinocytotic vesicles. However, it is now well established that the transendothelial pathway for aqueous transfer into the lumen of Schlemm's canal is through the transcellular channels of the giant vacuoles (see Tripathi & Tripathi, 1982 for review). The pressure-dependent nature of giant vacuoles has been clearly established in primates (Johnstone & Grant, 1973; Grierson & Lee, 1974, 1975*a*, *b*; Kayes, 1975) and in rabbits (Grierson *et al.* 1986), although in the latter study the response was less convincing due to problems of anatomical dissimilarity and variation in the organisation of the rabbit's angular aqueous plexus.

The present study has shown that the rat aqueous outflow system responds to various levels of experimentally induced intraocular pressure in a similar fashion to primates. At low IOPs the cribriform layer was compressed and giant vacuoles in the lining endothelium were rare. This is similar to the situation described by other workers in primates (Johnstone & Grant, 1973; Grierson & Lee, 1975*a*, *b*; Kayes, 1975; Van Buskirk, 1982). As intraocular pressure was increased the ciliary cleft, the spaces of Fontana and intertrabecular spaces widened. The cribriform layer was distended and there was a statistically significant increase in the number of giant vacuoles. Although there was clearly an overall trend there was some variation in the response, which was most noticeable at 10 and 40 mmHg. Several factors could account for this variation. Firstly, the small size of Schlemm's canal and the consequential low incidence of vacuoles per section may suggest that more extensive sampling from each eye and measurement of vacuole dimensions, possibly at the ultrastructural level, would be more appropriate quantitative methods. Another source of variation between animals may be poor sealing around the cannulation site, although no fluorescein leakage was observed. The unusually high numbers of giant vacuoles in at least one eye at 10 mmHg may be due to a possible delay in the fixative reaching the inner wall of Schlemm's canal until after death, whereupon with loss of central venous pressure (and therefore pressure within the canal) the differential across the endothelium during fixation would have been 10 mmHg. The slow penetration of fixative observed during the experiments at this pressure would support this, whereas at 20–40 mmHg the fixative quickly entered the eye and would most probably have reached the canal wall in the first 10 minutes while the animal was alive and there was still pressure within the lumen. Consequently the pressure differential across the endothelium during fixation, in for example eyes fixed at 20 mmHg, may have been only 10 mmHg. At higher pressures (20–40 mmHg), areas of focal endothelial detachment were more extensive in some eyes and therefore could possibly have accounted for some of the variation in the vacuolar incidence at higher pressures (especially 40 mmHg), particularly since it is well accepted that the detached endothelial monolayer is incapable of vacuolation (Svedbergh, 1976; McMenamin & Lee, 1986). The present study provides further evidence of the rapidity with which the lining endothelium responds to alterations in IOP and reinforces the need for its strict control during fixation in future studies of these tissues (McMenamin & Lee, 1986).

In contrast to the rabbit (Grierson *et al.* 1986) the rat outflow system is less prone to tissue damage at 40 mmHg. Admittedly this could be due to the delay of 1 hour before fixation in the study by Grierson *et al.* (1986), compared to 'immediate' fixation in the present investigation. Similarly 'wash-out' of extracellular material from the cribriform layer in the rat was also less evident than in previous primate studies (Grierson & Lee, 1975*a*, 1977*b*). This is probably due to the relatively good structural integrity of the tissue, which appears to be lost after an hour at high pressures (50 mmHg) (Grierson & Lee, 1975*a*) or prolonged exposure (4–5 hours) to mock aqueous humour at pressures within the normal range (McMenamin & Lee, 1986).

Relatively few complete transcellular channels in giant vacuoles were observed. This is probably due to the lack of serial sectioning and the small number of vacuoles along the short length of the canal in comparison to that in primates. A few giant vacuoles were noted in the walls of other vessels in the present study, especially those fixed at high IOPs. The phenomenon of giant vacuole formation as a means of draining aqueous may not be restricted to Schlemm's canal in the rat iridocorneal angle but may occur in the endothelium of other vessels if a sufficient pressure differential exists between the lumen and the anterior chamber.

The parallels between aqueous humour and cerebrospinal fluid in relation to their production, circulation, hydromechanical function and, in particular, the mechanisms of drainage are well known (see Tripathi, 1977). A full consideration of the debate is beyond the scope of this discussion. Interestingly, however, in a recent study in primates the giant vacuoles in the endothelial covering of the arachnoid villi, which several authors believe are morphologically and functionally identical to those in the endothelium of Schlemm's canal, have convincingly been shown to respond to experimentally controlled pressure differentials (Levine, Povlishock & Becker, 1982). These authors concluded that the behaviour of the vacuoles together with the size of the pores (1–2 μm) correlated well with the known physiological evidence of CSF absorption.

The findings of the present study provide encouraging evidence that the outflow tissues of the rat are pressure-sensitive and function in a similar manner to those of primates. Interestingly the work of Remé *et al.* (1983*a*, *b*) shows that the pre- and postnatal development of the rat chamber angle is similar to that of the human eye (Remé & Lalive d'Epinay, 1981). Van der Zypen (1977) injected substances such as ink, goldsol or horseradish peroxidase into the anterior chamber of rats and reported that this caused 'activation' of TECs. Although no mention was made of the time lapse between injection and enucleation, his observations do suggest that the TECs of rats possess phagocytic capability as in other species (see Lee & Grierson, 1982 for review).

Apart from the evidence that the outflow pathways in the rat are developmentally, morphologically and functionally similar to those of primates, this species also has the obvious advantages of being more convenient and less expensive. The technical difficulties presented by the small size of the rat eye and the shallow anterior chamber have presumably deterred previous experimentation on this species. These were overcome in the present study by use of a stereotaxic frame, micromanipulator and fine gauge needles. However, it is accepted that the size of the globe probably precludes the use of this species for more complex physiological manipulations. Otherwise the results of the present investigation are encouraging and suggest that this species may prove a valuable experimental model in the investigation of the normal and abnormal functional morphology of the aqueous drainage pathways.

SUMMARY

The eyes of 20 normal mature Swiss albino rats were fixed by intracameral perfusion with glutaraldehyde at various levels of intraocular pressure (10, 20, 30 and 40 mmHg). The anterior chamber was connected by a fine cannula to a reservoir of fixative for 10 minutes while the animal was maintained under anaesthesia for a further 20 minutes after death. Five animals were studied at each pressure. Fixation at 0 mmHg was achieved by rapid immersion of enucleated eyes from 5 animals whose eyes had been cannulated and open to atmospheric pressure for the first 10 minutes. The anterior segment tissues were studied by light microscopy and by scanning and transmission electron microscopy. The eyes from rats fixed by cardiac perfusion provided control tissue.

Progressive increase in intraocular pressure produced varying degrees of structural alterations in the iridocorneal angle. These included widening of the ciliary cleft and enlargement of the spaces of Fontana; however, the pectinate ligaments remained intact even at the highest pressure. The trabecular tissues became more distended and there was a statistically significant relationship between the fixation pressure and the mean number of giant vacuoles in the inner wall of Schlemm's canal. The response between animals fixed at the same pressure was variable. This was most pronounced at 10 and 40 mmHg. The results indicate that the rat outflow system responds morphologically to various levels of experimentally induced intraocular pressure in a similar fashion to primates. These findings, together with the morphological similarities between the rat and primate aqueous humour outflow pathways, particularly the presence of a single canal of Schlemm, suggest that the rat may be a valuable model for future studies of the normal and abnormal mechanisms of aqueous drainage.

The technical difficulties of experimental studies of the aqueous drainage mechanism in such a small eye are discussed.

This work was supported by the W. H. Ross Foundation (Scotland) for the Study of the Prevention of Blindness.

REFERENCES

ANDERSON, P. J., WANG, J. & EPSTEIN, D. L. (1980). Metabolism of calf trabecular (reticular) meshwork. *Investigative Ophthalmology and Visual Science* **19**, 13–20.

GRIERSON, I. & LEE, W. R. (1974). Changes in the monkey outflow apparatus by light microscopy and scanning electron microscopy. *Experimental Eye Research* **19**, 21–33.

GRIERSON, I. & LEE, W. R. (1975*a*). The fine structure of the trabecular meshwork at graded levels of intraocular pressure. (1) Pressure effects within the near physiological range (8–30 mmHg). (2) Pressure outside the physiological range (0–50 mmHg). *Experimental Eye Research* **20**, 505–521; 523–530.

GRIERSON, I. & LEE, W. R. (1975*b*). Pressure-induced changes in the ultrastructure of the endothelium lining Schlemm's canal. *American Journal of Ophthalmology* **80**, 863–884.

GRIERSON, I. & LEE, W. R. (1977*a*). Light microscopic quantitation of the endothelial vacuoles in Schlemm's canal. *American Journal of Ophthalmology* **84**, 234–246.

GRIERSON, I. & LEE, W. R. (1977*b*). Pressure effects on the distribution of extracellular materials in the rhesus monkey outflow apparatus. *Albrecht von Graefes Archiv für klinische und experimentelle Ophthalmologie* **203**, 155–168.

GRIERSON, I., NAGASUBRAMANIAN, S., EDWARDS, J., MILLAR, L. C. & ENNIS, K. (1986). The effect of various levels of intraocular pressure on the rabbit's outflow system. *Experimental Eye Research* **42**, 383–397.

HERNANDEZ, M. R., WEINSTEIN, B. I., WENK, E. J., GORDON, G. G., DUNN, M. W. & SOUTHREN, A. L. (1983). The effect of dexamethasone on the *in vitro* incorporation of precursors of extracellular matrix components in the outflow pathway region of the rabbit eye. *Investigative Ophthalmology and Visual Science* **24**, 704–709.

JOHNSTONE, M. A. & GRANT, W. M. (1973). Pressure-dependent changes in structures of the aqueous outflow system of human and monkey eyes. *American Journal of Ophthalmology* **75**, 365–383.

KAYES, J. (1975). Pressure gradient changes on the trabecular meshwork of monkeys. *American Journal of Ophthalmology* **79**, 549–556.

LEE, W. R. & GRIERSON, I. (1982). Anterior segment changes in glaucoma. In *Pathobiology of Ocular Disease* (ed. E. Garner & G. K. Klintworth), pp. 525–551. New York: Marcel Dekker.

LEE, W. R., GRIERSON, I. & McMENAMIN, P. G. (1982). The morphological response of the primate outflow system to changes in pressure and flow. In *Basic Aspects of Glaucoma Research* (ed. E. Lutjen-Drecoll), pp. 123–139. Stuttgart: Schattauer.

LEVINE, J. E., POVLISHOCK, J. T. & BECKER, D. P. (1982). The morphological correlates of primate cerebrospinal fluid absorption. *Brain Research* **241**, 31–41.

McMENAMIN, P. G. & LEE, W. R. (1986). Effects of prolonged intracameral perfusion with mock aqueous humour on the morphology of the primate outflow apparatus. *Experimental Eye Research* **43**, 129–141.

OHNISHI, Y. & TANIGUSHI, Y. (1983). Distributions of ^{35}S-sulfate and ^{3}H-glucosamine in the angular region of the hamster: light and electron microscopic autoradiography. *Investigative Ophthalmology and Visual Science* **24**, 697–703.

REMÉ, CH. & LALIVE D'EPINAY, F. (1981). Periods of development of the normal human chamber angle. *Documenta ophthalmologica* **51**, 241–268.

REMÉ, CH., URNER, U. & AEBERHARD, B. (1983*a*). The development of the chamber angle in the rat eye. I. Morphological characteristics of developmental stages. *Albrecht von Graefes Archiv für klinische und experimentelle Ophthalmologie* **220**, 139–153.

REMÉ, CH., URNER, U. & AEBERHARD, B. (1983*b*). The occurrence of cell death during the remodelling of the chamber angle recess in the developing rat eye. *Albrecht von Graefes Archiv für klinische und experimentelle Ophthalmologie* **221**, 113–121.

RICHARDSON, T. M., MARKS, M. S., AUSPRUNK, D. H. & MILLER, M. (1985). A morphologic and morphometric analysis of the aqueous outflow system of the developing cat eye. *Experimental Eye Research* **41**, 31–51.

ROHEN, J. W. (1982). The evolution of the primate eye in relation to the problem of glaucoma. In *Basic Aspects of Glaucoma Research* (ed. E. Lutjen-Drecoll), pp. 3–33. Stuttgart: Schattauer.

RUSKELL, G. L. (1961). Aqueous drainage paths in the rabbit. A neoprene latex cast study. *Archives of Ophthalmology* **66**, 861–870.

SVEDBERGH, B. (1976). Aspects of aqueous humour drainage. *Acta Universitat Uppsala* **256**, 1–71.

TRIPATHI, R. C. (1977). The functional morphology of the outflow systems of ocular and cerebrospinal fluids. *Experimental Eye Research* **25** (*Suppl.*), 65–116.

TRIPATHI, R. C. & TRIPATHI, B. J. (1972). The mechanism of aqueous outflow in lower mammals. *Experimental Eye Research* **14**, 73–79.

TRIPATHI, R. C. & TRIPATHI, B. J. (1982). Functional anatomy of the anterior chamber angle. In *Ocular Anatomy, Embryology and Teratology* (ed. F. A. Jakobiec), pp. 197–284. Philadelphia: Harper & Row.

VAN BUSKIRK, E. M. (1979). The canine eye: the vessels of aqueous drainage. *Investigative Ophthalmology and Visual Science* **18**, 223–230.

VAN BUSKIRK, M. E. (1982). Anatomic correlates of changing aqueous outflow facility in excised human eyes. *Investigative Ophthalmology and Visual Science* **22**, 625–632.

VAN DER ZYPEN, E. (1977). Experimental morphological study on structure and function of the filtration angle of the rat eye. *Ophthalmologica* **174**, 285–298.